

**ABSTRACT**

In this work, porous silicon (PSi) based gas sensor of structure (AL/nPSi/n-Si/AL) at different morphologies was prepared on the n-type silicon substrate using IR illuminated source of wavelength (810nm). The morphological and gas sensing properties of the sample were studied, under various etching time (5-20min). The current density –voltage characteristic at temperature from 25 to 150 °C of the sensor, which was sensitivity analysis based on the silicon nano size, porosity, layer thickness, and effective dielectric constant of the PSi layer. The SEM image of the PSi layer showed the formation single layer structure pore –like the cylindrical and rectangular pore shape. The porous layer after etching time (5-10min) and double of mud \_like for 20min produced different dimensions with randomly distributed as an upper layer and pore \_like structure as a lower layer. The current density–voltage analysis confirms that higher temperatures with the presence of CO<sub>2</sub> gas lead to sharply increase the sensitivity with the current and voltage. Overall, the improvement that appeared on the double porous layer sensitivity due to the higher value of the surface area.

**KEYWORDS:** porous silicon, surface morphology, gas sensor, carbon dioxide.

**INTRODUCTION**

Porous silicon (PSi) is considered as a very efficient material in the chemical sensor due to its unique properties which dependent on the large surface area [1]. That change in morphology of porous silicon can be obtained by the variety of etching condition through several parameters such as current density, etching time, HF acid concentration and illumination conditions. [2]. photo electrochemical etching of silicon by using HF acid is a well-known technique for porous silicon fabrication. The electrochemical and photochemical etching method is a combination of the material interaction with the HF acid through light and current density. It has been used laser light illuminating on the silicon electrode during the anodization process and was effect its greatly in modifying of the macro-porous properties [3]. That control of the high surface area within a small volume of the pore sizes given an increase in sensor characteristics. The ability to modulate dielectric constant as a function filling molecules makes of the PSi a suitable dielectric material for the gas detection process [4]. All these features lead to consider the PSi as one of the most valuable materials in the field of gas sensor technology. The PSi sensor is simple and cheap method as compared to other gas detectors that are super-sensitive could be based on PSi elements resistive [5]. The morphology and a reduced particle size play a significant role in the gaseous sensor applications, due to the increase of the specific surface area. On the other hand, PSi sensitivity is dependent also on the chemical adsorption and the physical adsorption of the gasses [6, 7]. The detection of carbon dioxide currently used in critical fields such as indoor air quality monitoring [8, 9]. The sensing devices Most of the currently available carbon dioxide are based on optical principles but they are usually bulky and expensive. In this research has been a study of several development groups in the alternative sensor for CO<sub>2</sub> monitoring which is cheap and efficient. The semiconductor materials are always a competitive low-cost choice in many areas [10]. In this research was the study focus on the porous silicon morphology on the CO<sub>2</sub> gas detection process. The electrical behavior in the sensing properties of (AL/nPSi/n-Si/AL) has been investigated at different temperature with the morphologies of the PSi layer.

**EXPERIMENTAL WORK**

**1-sample preparation**

The porous silicon gas sensor was fabricated using n-type silicon substrate of (100) orientation, and resistivity of about (10Ω.cm). The silicon wafer has been cut by dimensions at (2.4×2.4 cm), which is a fit with the size of the container. The porous silicon samples were prepared by using photo-electrochemical etching (PECE). The wafer surface has been cleaned by using the ethanol solution. It has been the solution of HF: Ethanol by rate (1:1) in the etching process of the silicon. The metal touch with silicon wafer acts as the anode, and it was inserted between the upper and the lower portions of Teflon cell (container cavity). The cathode was the circular shape of Platinum (Pt) and immersed in HF electrolyte. The cathode was held in place by the top part of the Teflon cell and textured by O-ring Plastic. The CW laser type at the wavelength of (810nm), the intensity (2W/cm<sup>2</sup>) at different etching times of (5,10 and 20 min) were used as shown in figure (1).

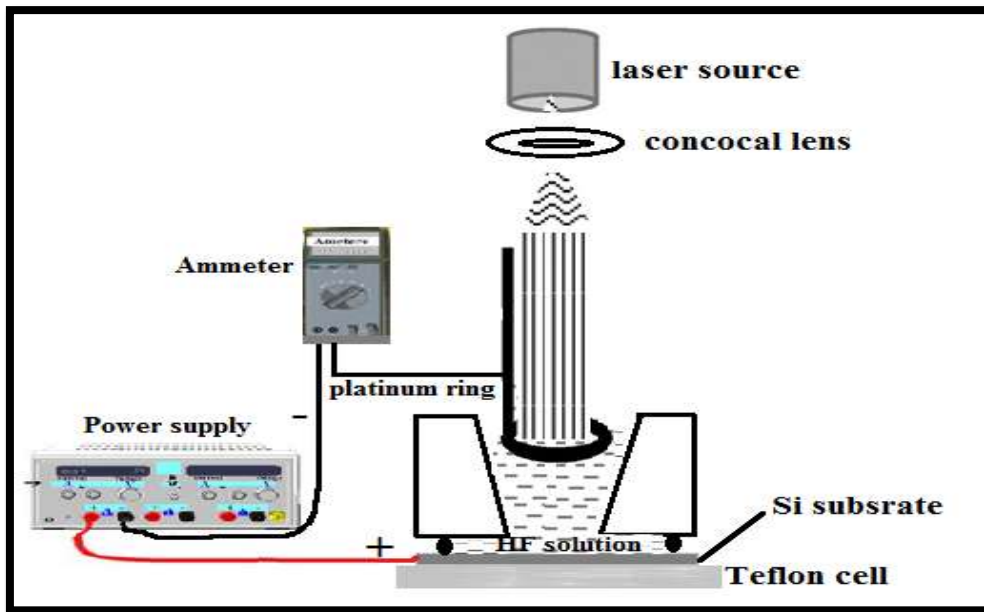


Figure (1): Show the experimental setup of PECE.

**2-Device fabrication**

After the final formation process of Psi layer required prepared Aluminium film as the electrode in order to the gas sensor application. The Aluminum film deposited onto the porous silicon surface to conduct electrical conduction process. It has been chosen Aluminum because of their advantages such as corrosion resistance, high conductivity, and ease preparation. The deposit of the thin film is on the upper Psi surface at the thickness of (5-20nm), and the bottom layer of Psi surface from Aluminum as an electrode to look like a sandwich structure of (AL/nPSi/n-Si/AL) as shown in figure (2).

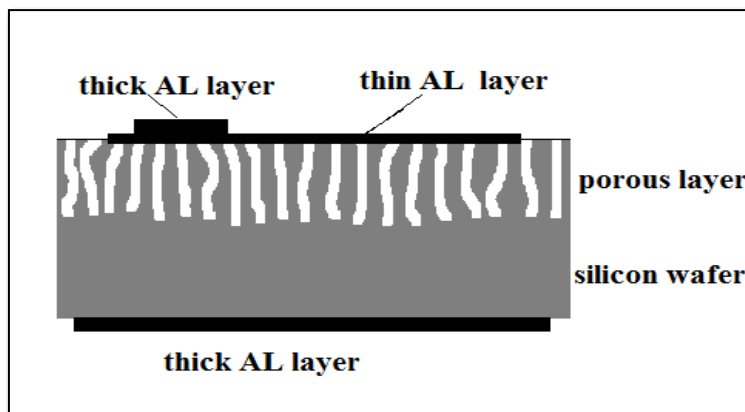


Figure (2) cross section of (AL/nPSi/n-Si/AL) structure gas sensor with electrical contact.

The J-V characteristic was made in the dark using DC power supply and electrometer device (Keithly 610C). The sensitivity of each sensor for detection was calculated.

**3-Gas exposure and measurements**

After deposited of the Aluminum electrode on the PSi sample, then exposed to 5ppm of CO<sub>2</sub> gas. The measurement has been used in this work at different temperatures 25, 50, 100, and 150 C°. The test chamber has the gas concentration which was controlled by changing the flow rate by using a mass flow controller. To ensure measurement accuracy were recorded after 1 minutes of turning on the gas flow in order to a homogeneous distribution of the gas under test in the chamber. For the purpose of comparison between the sensor behaviour, the sample has been exposed to dry air. Figure (3) represents the setup of measure the porous silicon sensor performance. The J-V characteristic was performed in a small sealed dark chamber with inlet and outlet to gas detection.

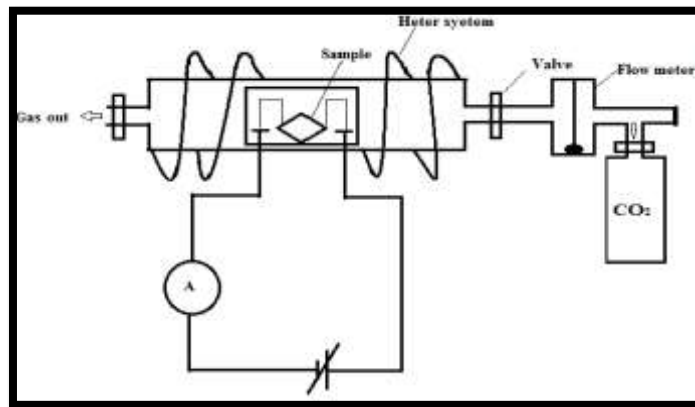


Figure (3) schematic diagram of the experimental setup for the sensing measurement.

**RESULT AND DISCUSSION**

**1-Porosity and layer thickness**

The porosity (p%) and layer thickness (d) are a very limiting parameter of Psi layer. They determined by gravimetric method according to following equations (1,2)[11].

$$P = (M_1 - M_2) / (M_1 - M_3) \dots \dots \dots (1)$$

$$d = (M_1 - M_3) / (\rho \times A) \dots \dots \dots (2)$$

Where M1 and M2, the sample mass before, after porous silicon formation respectively, M2 is the mass after complete dissolution of the porous layer, ρ is the density of bulk silicon (g/cm<sup>3</sup>) and A is the area of the porous silicon layer (cm<sup>2</sup>). The masses M2 and M3 are measured after drying the samples properly in the vacuum environment. The value of the porosity and layer thickness for each etching time was calculated for different porous silicon samples, and standard deviation of error bar is about 5%. The relation between porosity and layer thickness with etching time is shown in figure (4).

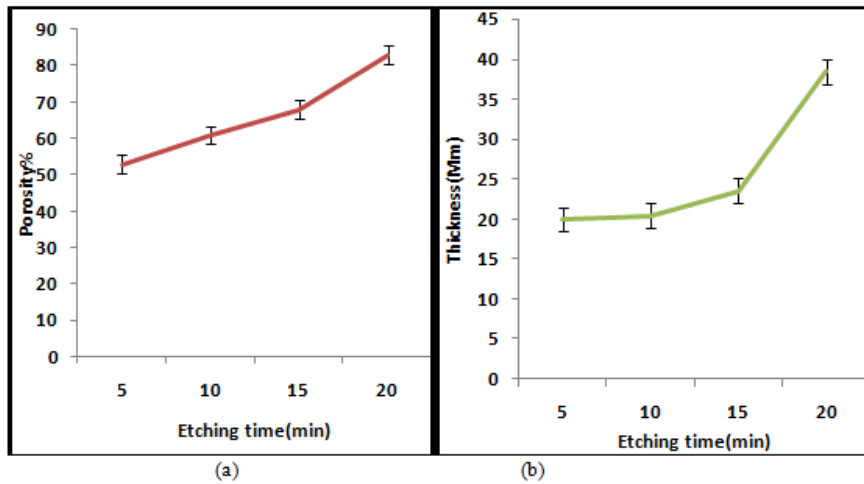
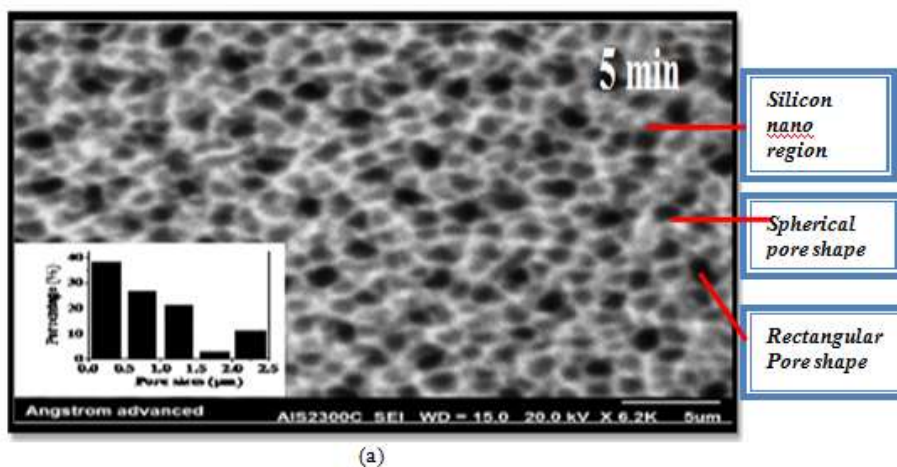


Figure (4): The (a) porosity (b) layer thickness of the porous silicon as a function to the etching time.

From figure (4a) the porosity increases linearly with increase the etching time reaching to the high value of about 83% at 20 min. The increasing of etching time to higher value than 20 min, the Psi layer become fragile and low mechanical properties. The relationship between the layer thickness and the etching time is shown in the figure(4b). The value of the Psi thickness layer increases with increase etching time, the higher value of the layer thickness is about (38.43 $\mu\text{m}$ ) at 20min etching time, the layer thickness has high value due to the increasing of the absorption depth for (810nm), where the absorption depth is about (12.9 $\mu\text{m}$ ). The wavelength of laser increase the penetration depth of incident photons, and the etching will occur at a region away from the porous layer, and inside the dark silicon regions so much greater e-h pairs will be generated, and this will increase the silicon dissolution process [12].

### MORPHOLOGICAL PROPERTIES

The critical of morphological properties is related to monitoring the nano size of the pore, how the channel distributed, and the channel conductivity [13]. The morphological properties of the result and porous layer like pore shape, pore width, and the wall thickness between the adjacent pores are strongly dependence on the etching parameter especially the etching time and illumination wavelength. These properties of (Psi) have been investigated by direct imaging of the structure by using Scanning Electron Microscope (SEM). The surface morphology of Psi sample of different etching times 5, 10 and 20 min as shown in figure(5). Based on the analysis of the SEM images figure(5a,b) the surface of the porous layer looks like pore \_like structure with different pore size and pore shape especially for the etching times(5, and 10min). At a high value of etching times, 20min and above the porous surface show dramatic changes in morphology, as shown in figure (5c).



(a)

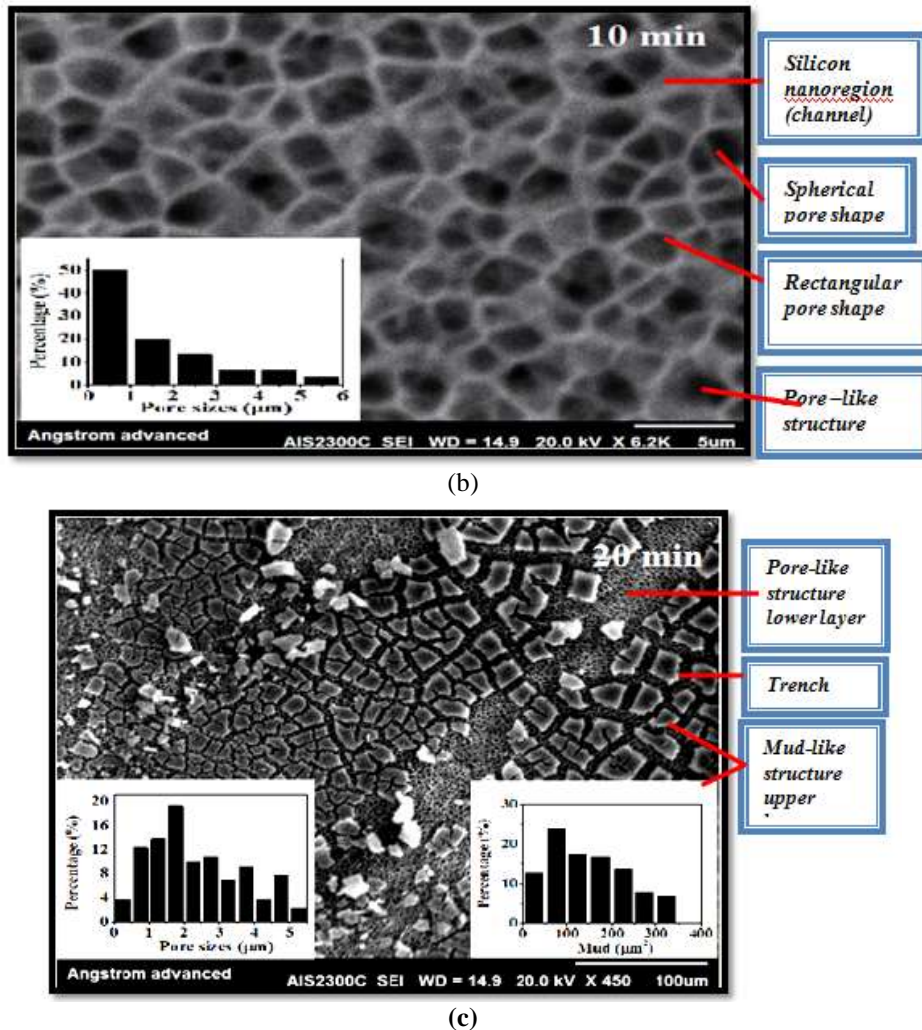


Figure (5) shows the SEM image of the porous sample at different etching time(a)5min (b)10minand(c)20 min

It has been observed the Psi layer possess approximate construction composed of mud \_like structure with different dimensions and randomly distributed as an upper layer and pore \_like structure as a lower layer at 20 min etching time. This complex double structure infrequently occurs and appears due to the excessive etching process at the surface of the silicon layer, which happens at the high etching current density or high etching time. In other hand, the starting edge of the electropolishing regime. The lower porous layer as stated early is pore \_like structure which represents the second step of the etching process which occurs after removing the first porous layer. The statistical distribution of mud in the upper porous layers and pores of the lower layer is illustrated in insight figure. The mud region varies from (0.1 to 400 μm<sup>2</sup>), and the peak of the distribution at (75μm<sup>2</sup>), and the pore size ranging from (0.1-5.5μm), and the peak of the distributed are about (2 μm). Figure (5b) shows the surface morphology of Psi layer after etching time at 10 min. Observations may be taken into account based on the;(i) pore size of the porous layer seems as a macropores Psi layer with different pore shapes nearly spherical and rectangular forms (ii) randomly distributed of the pores on the silicon surface. The significant value of the pore sizes may be attributed to increasing of e-h pairs within the porous layer, which enhance the silicon dissolution process between the nearest-neighbour pores.

The non-uniformity of Gaussian distribution of the laser beam intensity leads to make the etching rate has different values and hence resulting in a porous layer with different pore size. The statistical distribution of pore size across the Psi layer, which is pore width varies from (0.1 to 6 μm), and the maximum of the distribution was located at (0.5 μm). Figure (5a), which represent the surface morphology at 5 min etching time effects of increasing the etching time to (5, and 10 min) respectively. The comparing of the SEM images it appeared clearly with a less of

the etching time at about 5min. The surfaces topography of Psi layer still seems as a pore \_like structure with two kinds of pore a growth (i) some of the pores are completed growth and (ii) another of pores are non-completed growth the density on the non-completed pore is large than that of completed pores.

The forms of the pores are nearly spherical form these facts indicate that for lower etching time, the etching process will start in law rate, so the photogenerated charge carrier gets the small opportunity for initiating and growth of pores. On the other hand, by increasing the etching time to new value of about 10 min, the surface morphology of the pores layer, the density and the size of the completed growth pores is larger that of the non-completed growth. For 5min the statistical distribution of pores varies from (0.1to 2.5  $\mu\text{m}$ ) and the peak of the distribution located at(0.25 $\mu\text{m}$ ), and finally, for 10 min etching time, the statistical distribution of pores varies from(0.1 to 6  $\mu\text{m}$ ) and the peak of the distribution located at(0.5 $\mu\text{m}$ ).The increasing of the etching time will improve the silicon dissolution mechanism due to increasing the amount of the photo-generated e-h pairs and hence the pore size the pores overlapping process leading to synthesis the rectangular form (pores).

**PHOTOLUMINESCENCE STUDIES**

Photoluminescence studies of Psi layer were carried out using He-Cd laser system operating at 325nm wavelength. The( PL) spectra of porous silicon prepared with different etching times(5,10, and 20min) are shown in figure (6). The PL spectra of Psi were dominated by robust and broad emission peak spanning over a large part visible region from (500-750). The emission is attributed to the radiation carrier recombination process in the silicon nano-region.

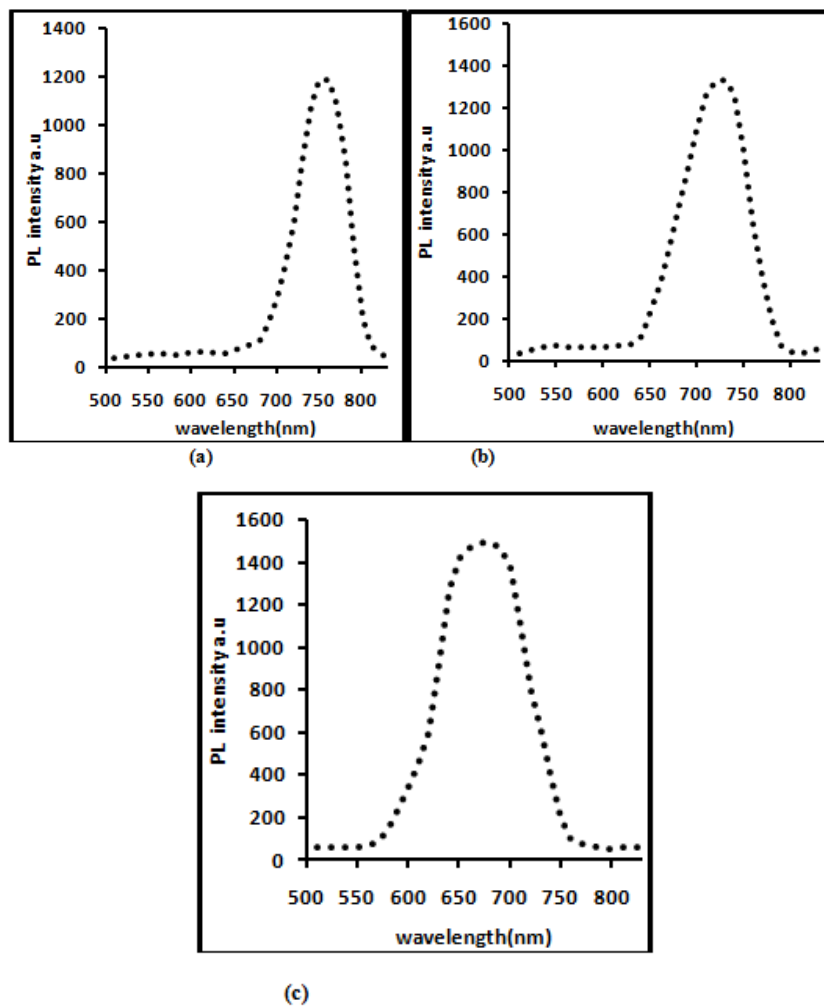


Figure (6): illustrates the PL spectra at different etching time, (a) 5min, (b) 10min, and (c) 20min

As shown from the figure (6) with increasing etching times 5, 10, and 20min, the PL spectrum resulted in an emission peak at a wavelength of 750,720, and 675nm respectively. The PL intensity is increasing with increasing the etching time with a blue shift in the PL peak position. The PL spectra with low PL intensity are due to the presence of bigger Si Nano crystal size in the porous layer. The average of the silicon nanocrystallite, energy gap of the porous layer, the peak of PL intensity and emission are showed in the table (1).

From the PL curve, the band gap of Psi and the Nano size were calculated from the equations (3,4)[14].

$$E_{g(Psi)} = hc/\lambda_{max} \dots \dots \dots (3)$$

Where h is plank constant, c is the light speed, and  $\lambda_{max}$  is obtained from the PL curve and then can determine the nano size L according to the following equation.

$$E_{g(Psi)} = E_{g(Si)} + 88.34/L^{1.37} \dots \dots \dots (4)$$

*Table(1): Illustrates, PL emission wavelength, PL intensity, energy band gap, and silicon nano size as a function to the etching time .*

Etching time(min)	Wavelength (nm)	PL intensity (a.u)	EgPsi (ev)	Si Nano size(nm)
5min	752nm	1200	1.7	3.9
10min	720nm	1335	1.72	3.8
20min	675nm	1500	1.84	3.3

**DIELECTRIC CONSTANT**

Various assumptions about the pore morphology may lead to the different model predicting the variation of dielectric constant in Psi layer as a function of porosity is illustrated in figure (7a). According to reference[15], the dependence of the dielectric  $\epsilon_{Psi}$  on the porosity of the porous layer is given by (5).

$$\epsilon_{rPsi} = (1-P\%)\epsilon_{rSi}^{1/3} + P\%\epsilon_{r air}^{1/3} \dots \dots \dots (5)$$

Where  $\epsilon_{r psi}$  the dielectric constant of the porous layer P% porosity  $\epsilon_{rsi}$  dielectric constant of silicon,  $\epsilon_{r pore}$  dielectric constant in air space.

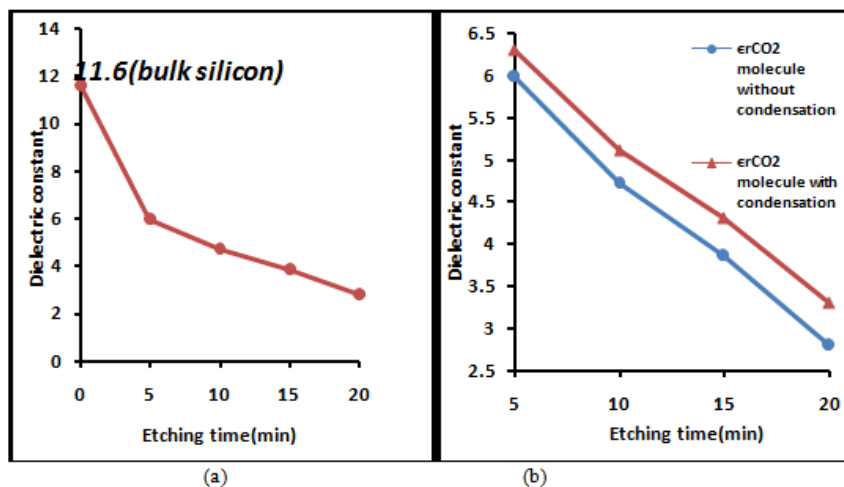


*Figure (7): The dielectric constant of Psi (a) air-filled Psi (b) CO2-filled Psi as a function to the etching time*

Figures (7) show the value of the silicon bulk dielectric constant is higher than that of Psi. The Psi layer is a new material different from bulk silicon, also found there mixed between two materials void space (air) and silicon channels. It clearly that some change happened in the  $\epsilon_r$  of Psi with the different etching times, that a reduction in dielectric constant due to the increase of dissolution process. On the other hand, the increasing of void space (air) and decreasing the silicon skeleton in the porous matrix is one of the desirable advantages. Figure (7b) shows the dielectric constant of the porous layer for the case of gas molecule –filled and condensed gas molecules –filled porous structure as a function of the etching time for porous silicon sample with different relative permittivity for CO<sub>2</sub>.

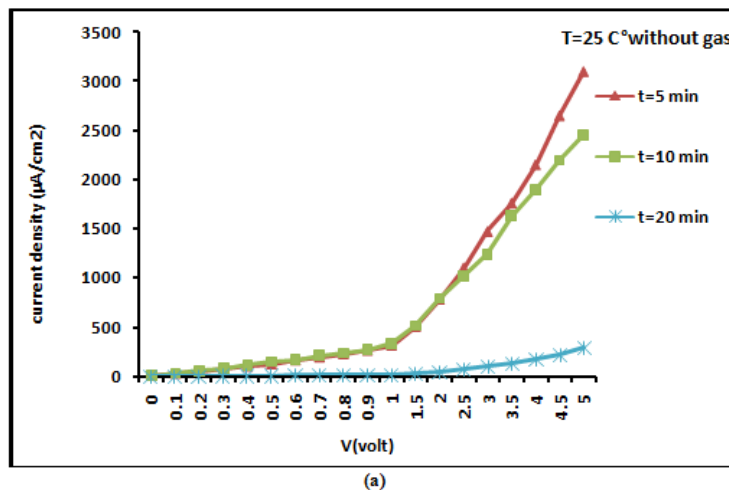
The condensation process of the matrix leads to increasing the effective dielectric constant for the porous matrix as shown Figure (7). The values of the dielectric constant for CO<sub>2</sub> molecule is about (1.000921) without condensation, and (1.6) with condensation [16]. The condensation process for the gas and vapor molecule in the porous structure occurred spatially in the micro and mesoporous silicon due to the capillary condensation of the adsorbate gas in the nanometer scale pores. The lower thermal conductivity of the porous layer improves the condensation process in the pores, where the Psi layer act as a heat insulator spatially when the pores are minuscule, and the porosity has higher value[17]. This modification in the dielectric constant of the porous matrix will lead to modifying over all electric and also the gas sensing properties.

### GAS SENSOR PROPERTIES

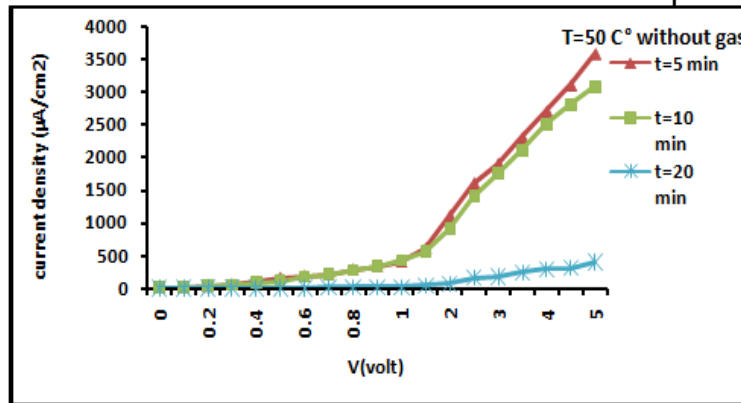
The sensing mechanism of this mode of operation is based on the response of the current density -voltage characteristic across the porous silicon /crystalline silicon junction. The performance of this junction as detection process varied according to the porosity and the porous layer (i.e energy gap of the porous layer) and the resistivity of the thickness of porous layer.

#### 5.1 Current density–voltage characteristic without gas

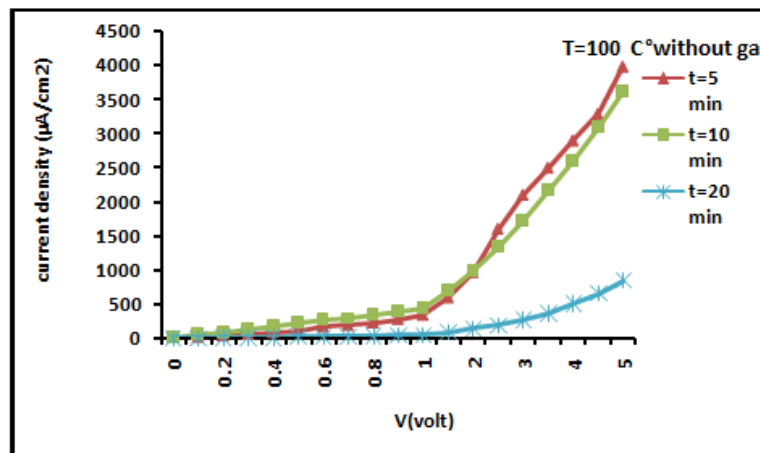
Figures (8 a ,b ,c ,d) show the J-V characteristics of porous silicon gas sensor in the sandwich (AL/ nPsi/n-Si/AL)structure at different temperatures 25,50,100,and 150C°. All measurement was taken in the dark at range of (0 - 5 v) with the case of absence of CO<sub>2</sub> molecule. The curve is typical of rectifying behavior for all porous silicon samples.



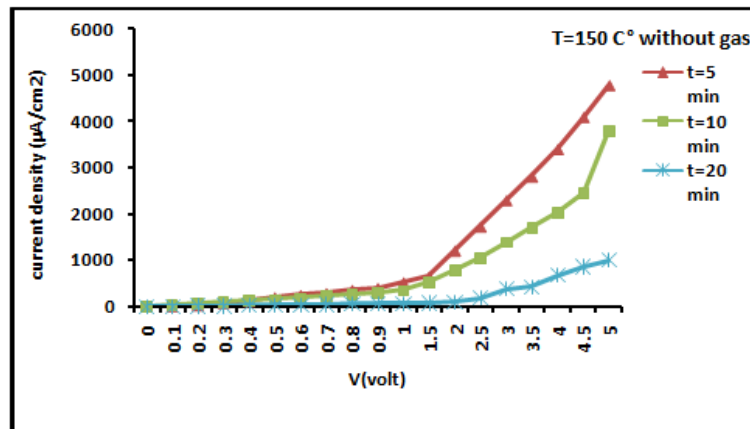




(b)



(c)



(d)

Figure (8): the  $J$ - $V$  characteristic for porous silicon gas sensor without gas at the different temperature (a)25,(b)50C°, (c)100,(d)150C°.

Overall, observe that the current was varied according to the porosity and the layer thickness of the porous layers and can be concluded the following factors:

At fixed temperature, the forward current passing through the fabricated sandwich structures decrease with increasing the etching times for both types of illuminated porous silicon samples. This behavior is due to the increasing the porosity and layer thickness with increasing the etching time, where the increasing of the porosity lead to decrease both of the dielectric constant of the porous silicon layer and the mobility of the charge carrier.

At fixed etching time the value of the current progressive increase slightly with increasing the operation temperatures from 25 °C to 150 °C.

The dependence of the forward current density of the layer thickness and porosity for both types of illumination are illustrated in figures(9).

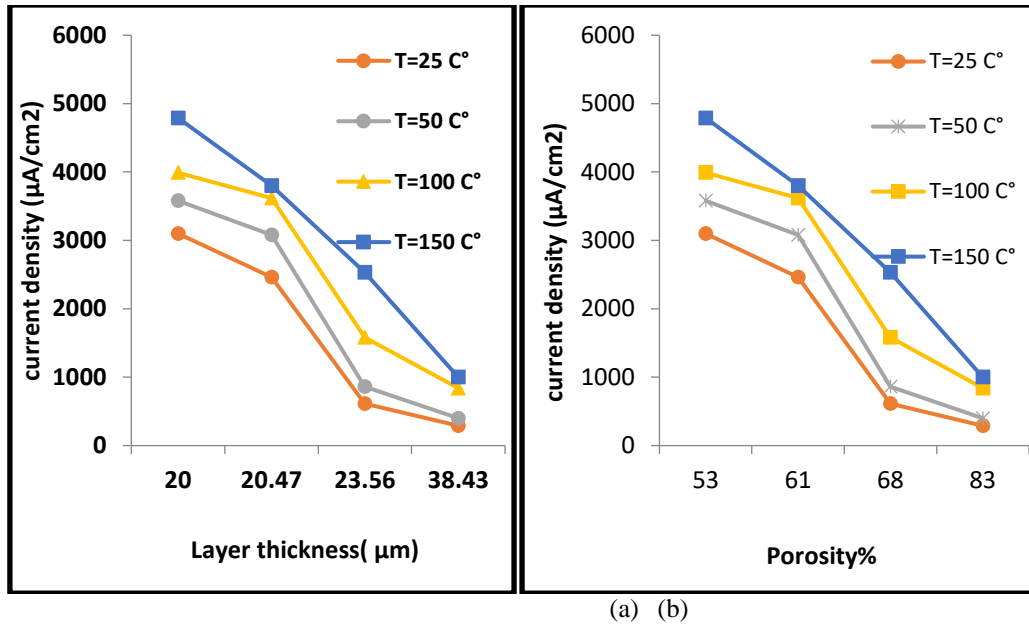


Figure (9): illustrates the forward current density at (5volt) as a function to the (a) porous layer thickness (b) porosity of Psi layer at different temperature

The variation of the current density passing through porous silicon is controlled by the depletion region inside the porous layer rather than the heterojunction between nPSi/n-Si. L.ABalogurovela [18]. They study the electrical properties of metal/Psi/C-Si structures with Psi layer of different thickness; they found out that the electrical properties of the structure with relatively thin (1μm)Psi layer significantly differ from those of solid structure in which the current flow is due to Psi/Si heterojunction.

In (AL/thick porous silicon /C-Si/AL) prepared device, the forward current density –voltage (J-V) behavior follows a power law relationship ( $J \propto V^2$ ) which indicates the space charge current attributed to the carriers drifting through the high resistivity luminescence porous silicon. In forward bias, the (J-V) characteristics exhibit a power-law relationship ( $J=kvm$ ) where k is a proportionality factor depended on the properties of the porous layer and  $m=2$  which implies that the total current of the device is dominated by carrier transport in the high resistivity Psi. In forward bias, electron and hole are injected into Psi layer. When the injected carrier concentration becomes comparable to the thermally generated concentration, the J-V characteristics of the device deviated from Ohmic behavior and the J-V relationship is [19]:

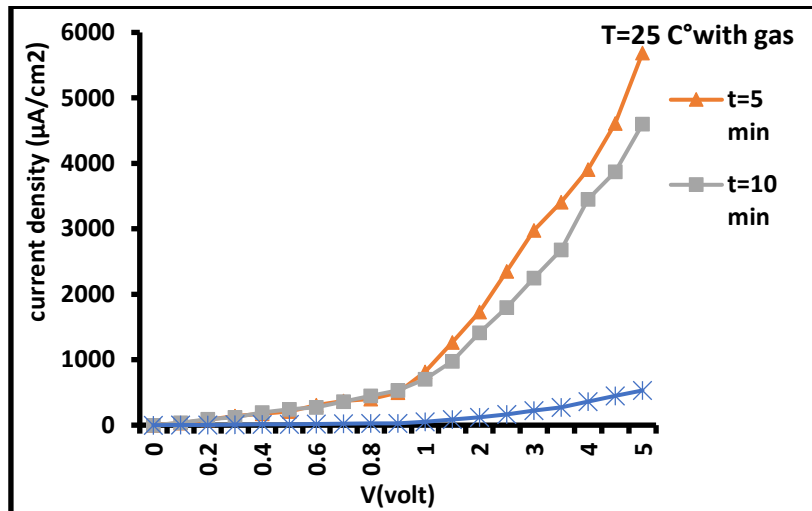
$$I_{PSi} = \epsilon_{rPSi} \epsilon_0 \mu_{eff} V^2 / d^3 \dots \dots \dots (6)$$

Where  $\epsilon_{rPSi}$  is a dielectric constant of PSi,  $\epsilon_0$  dielectric constant of vacuum,  $\mu_{eff}$  is the mobility, V the voltage, and d the layer thickness. The dielectric constant of the porous layer is related to the porosity of the porous layer and the filling gas of the pores. Furthermore, that have found the J-V characteristics depended on the temperature in the range from 25 °C to 150 °C.

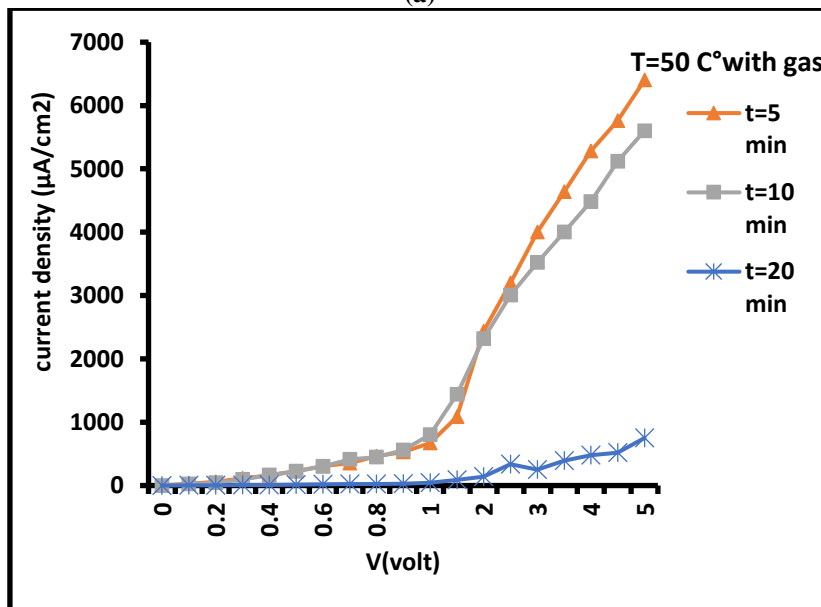
**5.2 Current density –voltage characteristic with gas**

Figure (10) present the J-V characteristics of gas sensor in the structure (AL/nPSi/n-Si/AL) at different temperatures 25,50,100,150C° under the pressure (5ppm) CO2. For both curves exposure to CO2 gas did not change the shape of J-V characteristic (still rectifying) but the values of the current at presence of CO2 gas is higher than that the case without gas, the variation in the current indicating that the sensor is very sensitive to CO2 gas. Figure show the variation of the current at maximum applied voltage +5V at fixed operation temperature

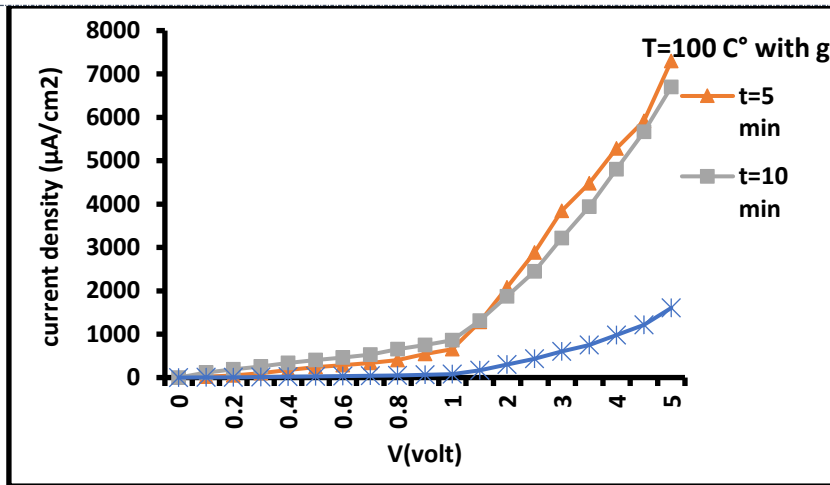
before and after is exposure to CO<sub>2</sub> gas increased with increasing the etching time. That means the fabricated sensor is very sensitive to morphological properties of the porous layer, porosity, layer thickness, and the increasing the etching time will increase the specific area (active sensitivity area). The increasing of the current density for all samples is related to the role of the CO<sub>2</sub> molecules where desorption of the molecule on the porous silicon layer due to the Vander Waals interaction will lead to modifying the dielectric constant of the porous layer. The presence of the CO<sub>2</sub> gas will enhance the current flow in the fabricated sensor. According to the [17], the CO<sub>2</sub> molecules act as an acceptor, which will lead to an increasing of the free carrier concentration.



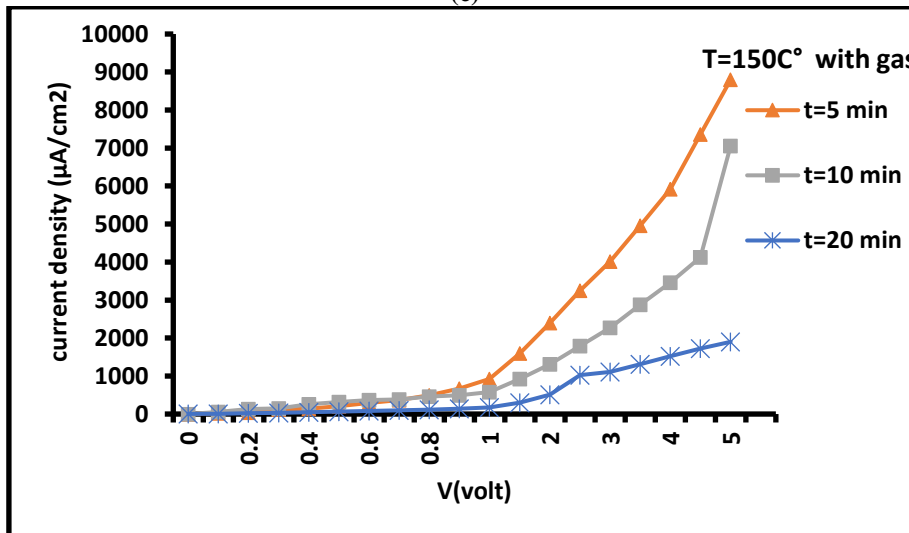
(a)



(b)



(c)



(d)

Figure (11):illustrated the J-V characteristics of porous gas sensor of structure (AL/nPSi/n-Si/AL)at different temperature (a)25 ,(b)50C°, (c)100, (d)150C° under CO<sub>2</sub> gas at pressure of ((5%)ppm .

### 5.3 Sensitivity

The gas responsively for gas detection device can be defined as the dramatical change in the current or other physical quantities of the sensor surface before and after exposure to the gas. The gas response is shown in the following equation [20].

$$S = \frac{I_a - I_g}{I_g} \times 100 = \frac{\Delta I}{I_g} \times 100\% \dots \dots \dots (7)$$

, I<sub>o</sub> the essential current of PSisensor in presence of atmospheric air, and I<sub>g</sub> is the current after exposure to gas.

The variation of the maximum detection sensitivity at fixed operating voltage 5V with operating temperature in the range from room temperature to 150C° of the porous layer as has shown a figure (12).

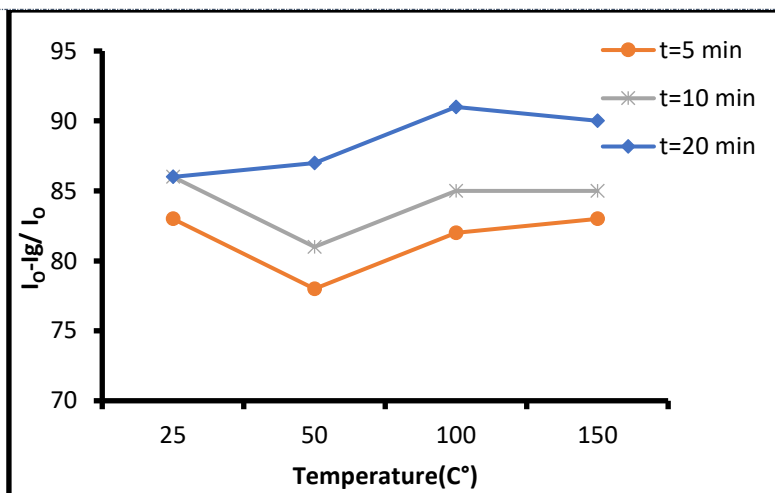


Figure (12): shows the variation of the sensitivity at 5V applied voltage for porous gas sensor of structure (AL/nPSi/n-Si/AL) with operating temperatures.

The temperature variations revealed the through current passing in the sensor device. It was found that the increase of the device sensitivity is correlative with the rise in the operating temperature from 50 and reaches a maximum to 150 C°. However, the increase of the porous sample which prepared at long etching time (low conductivity). That was higher than of the porous sample with low etching time (high conductivity). Overall, this indicates the fact that the optimum sample has high resistive, with double porous layer and hence a higher value of the specific surface area. That may be attributed as follows the rate of the adsorption of the CO<sub>2</sub> gas molecules on active porous layer increase with the rise in the operating temperature. The causes a rapid increasing in the passing charge carriers and hence an increasing in their sensitivity.

## CONCLUSION

Photoelectrochemical etching process fabricated the Psi based gas sensor substrate in (AL/nPSi/n-Si/AL) sandwich the sensitivity will modify according to the porous silicon morphology. Higher sensitivity was obtained with double porous layer morphology rather than the unique layer morphology for all operating temperature.

## REFERENCE

- [1] M. Draghici, M. Ciurea, V. Iancu, XLV - XLVI, *S. Fizica Stării Condensate*, Tomul, (1999, 2000) 86-90.
- [2] Jeyakumaran N., Natarajan B., Ramamurthy S. and Vasu V., "Structural and optical properties of n-type porous silicon-effect of etching time, *IJNN*, Vol.3, No.1, December, 2007.
- [3] R.K. Soni G.R. Bassam, S.C. Abbi, *Applied Surface Science* 214 (2003) 160.
- [4] L. T. Canham, "properties of porous silicon" INSPEC, England, (1998).
- [5] Anderson R.C., Muller R.S. and Tobias C.W. (1990) Investigation of porous silicon for vapor sensing. *Sensors and Actuators A*, 21, 835-39. 62.
- [6] V. Parkhutik, Porous silicon-mechanisms of growth and applications, *Solid State Electron.*, **43**, 1121 (1999).
- [7] R. C. Anderson, R. S. Muller, and C. W. Tobias, Investigation of porous silicon for vapour sensing, *Sensor. Actuator*. **A21-23**, 835 (1990).
- [8] K. Kaneyasu, K. Otsuka, Y. Setoguchi, S. Sonoda, T. Nakahara, I. Aso, N. Nakagaichi, A carbon dioxide gas sensor based on solid electrolyte for air quality control, *Sens. Actuators B* 66 (2000) 56-58
- [9] J- Frank, H. Meixner, Sensor system for indoor air monitoring using semiconduction metal oxide and IR-absorption, *Sens. Actuators B* 78 (2001) 298-302.
- [10] J. Herrón, G.G. Mandayo, E. Castano, Solid state gas sensor for fast carbon dioxide detection, *Sens. Actuators B* 129 (2008) 705-709.
- [11] Bisi, O., Ossicini, S. & Pavesi, L. (2000). Porous silicon: a quantum sponge structure for silicon based optoelectronics, *Surface science reports* 38: 1-126.
- [12] Matthew S. Brown and Craig B. Arnold, *Fundamentals of Laser-Material Interaction and Application to Multiscale Surface Modification*, Springer Series in Materials Science 135, DOI 10.1007/978-3-642-10523-4\_4.

- 
- [13] LEIGH CANHAM DERA, Malvern, U K, Porous Silicon, Published by: INSPEC, The Institution of Electrical Engineers, London, United Kingdom 1997.
- [14] Alwan M. Alwan, Narges Z. Abdulzahra, N. M. Ahmed, N. H. A. Halim, Influence of rapid thermal oxidation process on the optoelectronic characteristics of PSI devices, *Int. J. Nanoelectronics and Materials* 2 (2009) 157-161.
- [15] Peng C., Hirschman and K.D and Fauchet P M. *J.Appl.Phys*, 80 , 295, 1996.
- [16] "*Phase change data for Carbon dioxide*". *National Institute of Standards and Technology*. Retrieved 2008-01-21.
- [17] GG. Korotcenkov, Beongki K Cho, Porous Semiconductors: Advanced Material for Gas Sensor Applications, *CRITICAL REVIEWS IN SOLID STATE AND MATERIAL SCIENCES* · FEBRUARY 2010 · DOI: 10.1080/10408430903245369.
- [18] L.A.Balagurov, A. F. Orlov, B. unal and S. C Bayliss *Journul of Applied physics* vol90, no8 october2001.
- [19] S.M.sze "Semiconductor Devices –physics and technology" wiley, America(1985).
- [20] Y.-J. Choi, I.-S.Hwang, J.-G.Park, K.-J.Choi, J.-H.Park, J.-H.Lee, Novel fabrication of a SnO<sub>2</sub> nanowire gas sensor with high gas response. *Nanotechnology* 19, 095508 (2008).doi:10.1088/0957-4484/19/9/095508